Chapter 2

Third-Generation-Sensitized Solar Cells

Muhammad Ammar Mingsukang,
Mohd Hamdi Buraidah and Abdul Kariem Arof

Additional information is available at the end of the chapter

http://dx.doi.org/10.5772/65290

Abstract

The need to produce renewable energy with low production cost is indispensable in making the dream of avoiding undue reliance on non-renewable energy a reality. The emergence of a third-generation photovoltaic technology that is still in the infant stage gives hope for such a dream. Solar cells sensitized by dyes, quantum dots and perovskites are considered to be third-generation technological devices. This research focuses on the development of suitable and reliable sensitizers to widen electromagnetic (EM) wave absorption and to ensure stability of the photovoltaic system. This article discusses the basic principles and the progress in sensitized photovoltaics.

Keywords: third-generation solar cells, sensitized solar cells, dye-sensitized solar cells, quantum dot-sensitized solar cells, perovskite-sensitized solar cells

1. Introduction

Third-generation photovoltaics are able to produce high efficiency photon to electricity conversion devices at a cheaper production cost. Solar cells based on pure Si forms were the first-generation devices with an efficiency of ~27%. Due to the high production cost, researchers searched for new processes and materials that led to the second-generation solar cells comprising copper indium diselenide, amorphous silicon, and polycrystalline solar cells. Production was still expensive, as the fabrication process required a large amount of energy. Production of the third-generation solar cell is cheaper and the cells are reasonably efficient. There are several technologies classified as third-generation solar cell technologies. These include solar cells sensitized by a dye material, solar cells sensitized by quantum dots (QDs) and perovskite-sensitized solar cells. These solar cells have a similar structure consisting of a

photoanode, counter electrode (CE) and a medium for charge transport. The working principle is also similar. Work on sensitized photovoltaics started during the 1970s with the use of organic dyes as the sensitizer. Organic dyes can be natural or synthetic. Natural organic dyes can be obtained from plant sources but the performance is poor and the efficiency is low. Apart from natural organic dyes, synthetic organic dyes can give efficiency as high as 13%. Ruthenium based dye is one of the synthetic organic dyes and is known to give good performance with current density about 20 mA cm^{-2}. As development in dye-sensitized solar cells (DSSCs) continues, an idea to replace organic dyes with inorganic sensitizers resulted in the emergence of quantum dot-sensitized solar cells (QDSSCs) that utilize quantum dots or nano-sized semiconductor crystals with a short band gap and a high extinction coefficient. Later, since 2009, researchers have begun to use perovskite materials as sensitizers. Perovskite works very well with the solid-state hole transfer material and until now its efficiency has reached 21%. However, perovskites are very moisture-sensitive materials and fabrication must be done in very clean and controlled conditions. In sensitized solar cells, the photoanode is a very crucial component because this is where the electrons are generated by the sensitizer. Photoanodes will absorb photons, excite and transport electrons when illuminated. On exiting the photoanode, the electrons will be sent to the cathode and returned to the sensitizer via a hole conductor or a redox mediator in the electrolyte. For DSSCs, the photoanode components are the dye sensitizer, a mesoporous semiconducting oxide layer and a transparent conducting oxide (TCO). Photoanodes for QDSSC and perovskite solar cells have similar components with DSSCs except that quantum dot nano-sized semiconductor crystals and perovskite materials act as the sensitizer. Another difference between them is the redox mediator used in the electrolyte. QDSSC works well with the polysulphide electrolyte instead of the iodide based electrolyte (as in DSSCs) because the iodide-based electrolyte will cause rapid degradation in photocurrent due to the corrosive nature of the iodide ion on many semiconductor materials including quantum dots. Perovskite solar cells use hole conductors instead of a redox mediator electrolyte. **Figure 1** illustrates progress of third-generation devices.

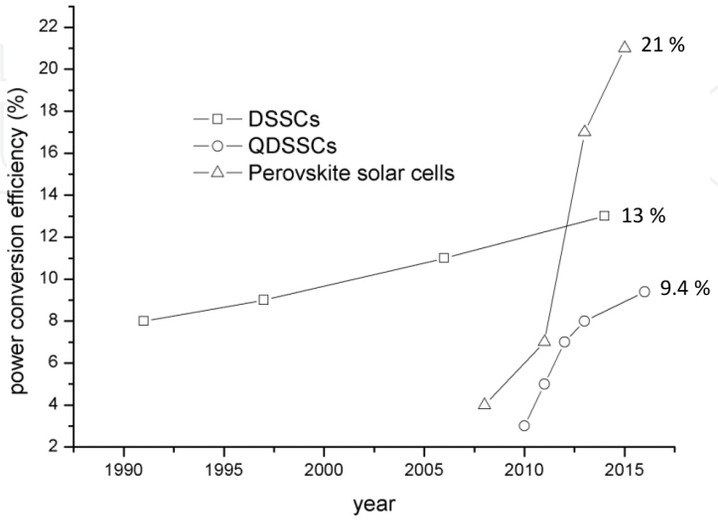

Figure 1. Graphs showing progress of third-generation photovoltaics.

2. Dye-sensitized solar cells (DSSCs)

DSSCs employ oxide semiconductors with wide band gaps and sensitizers that absorb electromagnetic (EM) waves in the visible light. DSSC was first developed in 1972 as a chlorophyll-sensitized zinc oxide (ZnO) electrode solar cell [1]. In 1976, an amorphous silicon photovoltaic was reported for the first time by Carlson and Wronski, and its efficiency was 2.4% [2]. Subsequently, solar energy researchers began to give attention to DSSCs. However, the main dilemma was that a single layer of dye molecules on the surface allowed only 1% incident sunlight absorption that delayed further progress [3]. The breakthrough in DSSC research was in 1991 [4]. The efficiency was 7.1%. About 80% of photons absorbed were converted into electrical current. The cheap cost of production and the simple structure inspired many researchers worldwide to improve the efficiency to a level deemed acceptable for commercialization.

The DSSC operating principle may be compared to the process of photosynthesis with the dye functioning as chlorophyll [4]. In DSSCs, the transport of charges (electrons) to the external circuit begins when electrons exit the semiconducting network layer and ends when the redox mediator in the charge transport medium returns them to the sensitizers. The purity of the semiconducting material is not as crucial as in the earlier generation solar cells.

2.1. DSSC structure

Figure 2 shows the structure of a DSSC. The photoanode consists of a TCO substrate on the top of which is deposited a semiconducting oxide layer (usually TiO_2) and the dye sensitizer. Actually, there are two TiO_2 layers. The first TiO_2 layer is a blocking layer to suppress electron recombining with the ionized dye and/or the mediators. The second layer is mesoporous TiO_2 of 20–30 nm thickness. These particles are larger than the blocking layer particles. The mesoporous TiO_2 layer thickness is about 10 μm. A colloidal TiO_2 paste for the

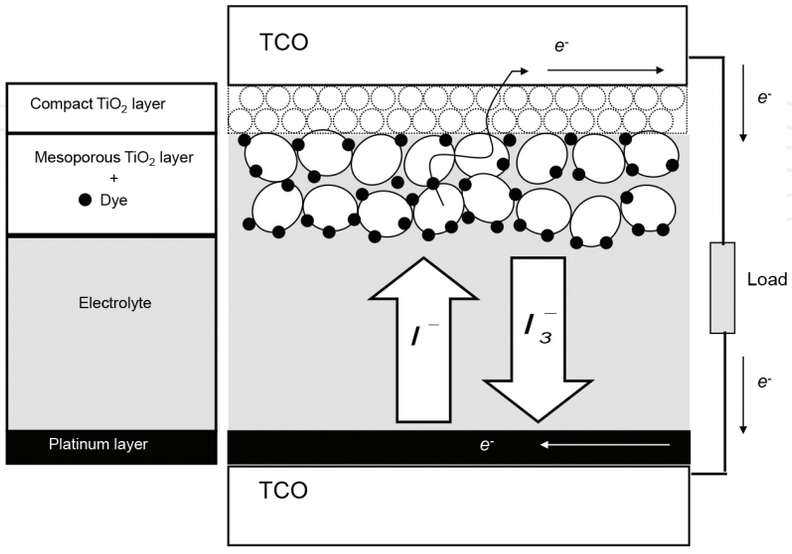

Figure 2. Schematic diagram of the DSSC structure.

second layer can be prepared by grinding TiO_2 of 21 nm size with nitric acid, a polymer of low molecular mass (e.g. polyethylene glycol of molecular mass 200 g/mol) with a little surfactant. This paste will be deposited over the blocking TiO_2 layer and heated at ~450°C for 30 min. To ensure the dye adheres to the mesoporous TiO_2 layer, the TiO_2 films are soaked in the dye solution overnight. The larger surface area of the mesoporous TiO_2 area allows a greater amount of dye to be adsorbed on its surface. An electrolyte usually with an iodide/triiodide couple is needed for DSSC. The electrolyte can be in liquid or gel form. A catalytic active material (usually platinum) is required as the counter electrode to reduce the triiodide ion (I_3^-) to the iodide ion (I^-).

2.2. Working principle of DSSCs

Figure 3 shows the energy levels in the working of a DSSC. The Fermi energy level of TiO_2 will be aligned with the redox energy level when there is no light. Upon illumination, dye molecules (*D*) attached to the mesoporous TiO_2 surface absorbs photons of energy, *hv*. Electrons in the highest occupied molecular orbital (HOMO) of the dye molecules will be excited into the lowest unoccupied molecular orbital (LUMO), see Eq. (1).

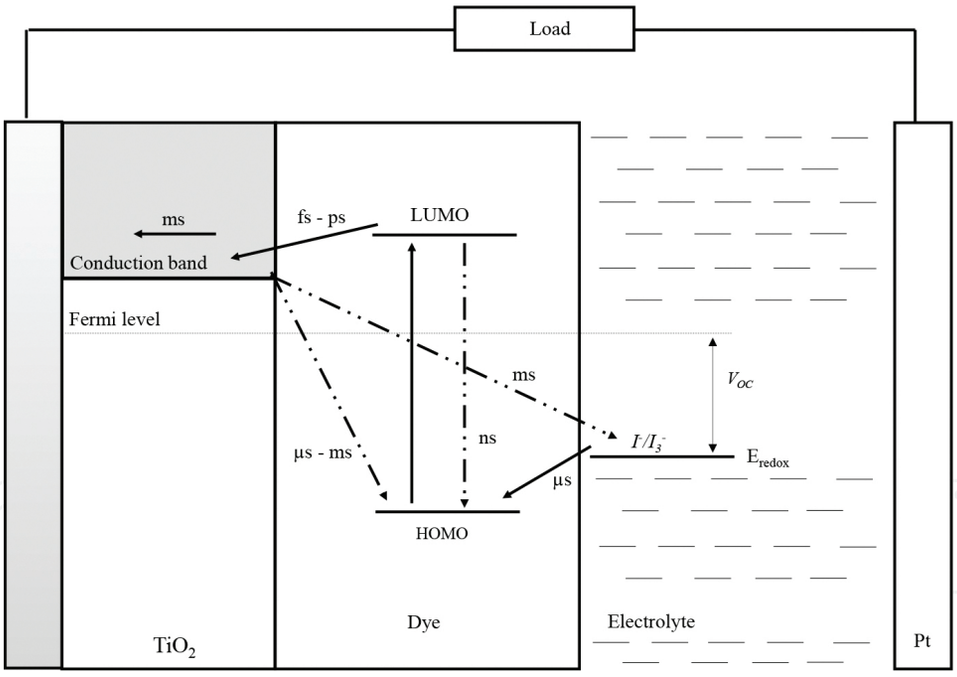

Figure 3. Schematic diagram showing the kinetic processes at the TiO_2/dye/electrolyte interface.

$$D + hv \rightarrow D^* \quad \text{light absorption} \tag{1}$$

Here, D^* is the excited dye molecule. Electrons in the LUMO of the dye will be transferred to the mesoporous TiO_2 within femtoseconds, ~10^{-15} s. This process is called electron injection.

The Fermi level of TiO_2 will be increased towards the conduction band (CB). The dye molecule is now in an oxidized or ionized state (D^+), Eq. (2). The difference in the potential between the Fermi and the redox levels will be manifested as the voltage of the device.

$$D^* \rightarrow e^-_{(TiO_2)} + D^+ \quad \text{electron injection} \tag{2}$$

The transferred electrons percolate through the interconnected nanocrystalline TiO_2 network to the conducting substrate within milliseconds (10^{-3} s). For good performance of the DSSC, this process has to be completed with the recombination reaction displayed in Eqs. (3) and (4).

$$e^-_{(TiO_2)} + D^+ \rightarrow D \tag{3}$$

$$2e^-_{(TiO_2)} + I_3^- \rightarrow 3I^- \tag{4}$$

Eq. (3) describes electron recombination with the ionized dye molecule and Eq. (4) describes electron-triiodide ion recombination. Electrons exit the TCO substrate and travel towards the counter electrode through the external circuit and reduce a triiodide ion in the electrolyte to an iodide ion as shown in Eq. (5).

$$\frac{1}{2}I_3^- + e^-_{(CE)} \rightarrow \frac{3}{2}I^- \tag{5}$$

The iodide ion diffuses to the photoanode and is oxidized back to a triiodide ion regenerating the dye molecule in the process. This process occurs continuously as shown in Eq. (6).

$$D^+ + \frac{3}{2}I^- \rightarrow D + \frac{1}{2}I_3^- \tag{6}$$

2.3. Dye sensitizer

The dye sensitizer is one of the important components of the DSSC. It works as an absorber of light and produces electrons. For good light conversion into electricity, the dye or sensitizer must have the following:

1. A broad absorbance spectrum of solar light for high photocurrent.
2. Anchoring groups such as carboxylate for attachment on the TiO_2 surface so that electron transfer can occur from the LUMO of the dye to the TiO_2 CB.

3. In order for the electrons to be transferred to the oxidized dye molecules efficiently for dye regeneration, the redox level has to be at more negative potential than the HOMO potential of the dye. The LUMO has to be less positive compared to the TiO_2 CB for electron injection.

4. The dye covering the TiO_2 surface should not stack on each other.

2.3.1. Ruthenium sensitizer

Desilvestro et al. [5] was the first to report the use of ruthenium complex tris(2,2′-bipyridyl-4,4′-di-carboxylate)ruthenium(II) dichloride dye in DSSC. The percentage conversion of absorbed incident photons to current (IPCE) for this DSSC was 44%. In 1991, O'Regan and Grätzel, reported IPCE of more than 80% from a DSSC using [Ru(2,2′-bipyridine-4,4′-dicarboxylicacid)$_2$(μ-(CN)Ru(CN) (2,2′-bipyridine)$_2$)$_2$] dye adsorbed on a mesoporous, nanocrystalline TiO_2 surface. The electrolyte contained I^-/I_3^- and the counter electrode was platinum [6]. The efficiency of the DSSC was more than 7%. Nazeeruddin et al. [7] have prepared several ruthenium(II) complexes. These sensitizers are cis-X_2bis(2,2′-bipyridyl-4,4′-dicarboxylate)ruthenium(II) dye sensitizers. X comprises halide anions, CN^- and SCN^-. The cis-di(thiocyanato)bis(2,2′-bipyridyl-4,4′-dicarboxylate) ruthenium(II) dye has been coded as N3. Among all the ruthenium complexes, N3 is a better sensitizer for charge transfer. N3 absorbs a wide wavelength range in the visible light. It has four carboxyl groups that strongly adsorb on the TiO_2 surface and has a long excited state lifetime. The IPCE value exhibits more than 80% between 480 and 600 nm. The electrons are injected into the TiO_2 CB via a metal-to-ligand charge transfer (MLCT) route as shown in **Figure 4**. According to Bryant et al. [8], the carboxylated complexes exhibit two $t_2 \rightarrow \pi^*$ MLCT bands in the near UV and visible region. The absorbance of Ru(2,2′-bipyridine-4,4′-dicarboxylicacid)$_2$(NCS)$_2$, i.e. N3 dye at visible region, $t_2 \rightarrow \pi^*$ is higher than other dihalogeno derivative dyes [7].

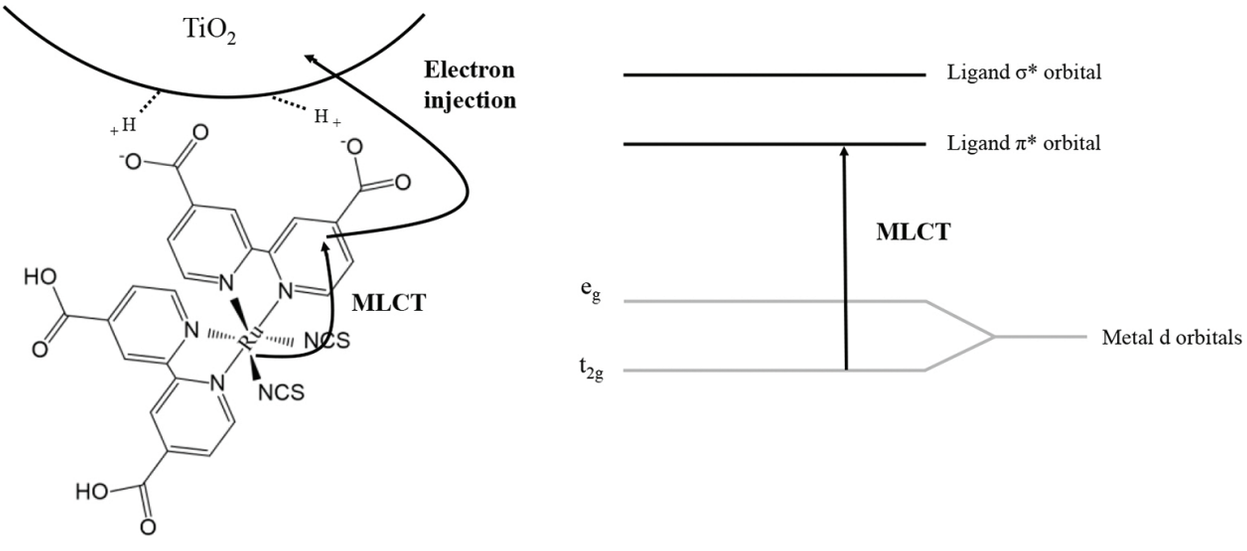

Figure 4. Charge transfer route from dye to TiO_2.

The N3 dye was almost no match in terms of charge transfer ability until Nazeeruddin et al. [9] developed the triisothiocyanato-(2,2′:6′,6″-terpyridyl-4,4′,4″-tricarboxylato) Ru(II) tris(tetrabutylammonium) or 'black dye' and coded as N749. The DSSC with black dye showed a broader IPCE spectrum in the visible region compared to N3. The overall efficiency obtained for this DSSC with black dye was 10.4% under 1 Sun illumination [10].

The substitution of two protons in the carboxyl group of N3 dye with tetrabutylammonium cations resulted in $[Bu_4N]_2[Ru(4\text{-carboxy-}4\text{-carboxylate-}2,2'\text{bipyridine})_2(NCS)_2]$ or N719 dye. This dye exhibits a higher efficiency than N3 dye [11]. The higher efficiency is related to the higher V_{oc} that resulted from the upshift of the TiO_2 Fermi level. However, the performance of DSSC using N719 dye is still lower than the N749 since N719 does not absorb in the red. To extend the EM absorption region, the dye can be tuned. This can be accomplished by introducing a π^* molecular orbital ligand and by using a strong donor ligand to destabilize the metal t_{2g} orbital [12]. By achieving this, the absorption range can be stretched from visible to the near infrared region. Islam et al. [12] have synthesized ruthenium complexes containing 2,2′-biquinoline-4,4′-dicarboxylic acid where the π^* orbital is lower or at a more positive potential than that containing 2,2′-bipyridine-4,4′-dicarboxylic acid. The DSSC using this sensitizer exhibited lower efficiency due to the dye excited state being at a more positive potential than the CB of TiO_2. This led to reduced electron injection driving force and lowered the photocurrent. The nanocrystalline TiO_2 soaked in $[Bu_4N]_2[cis\text{-}Ru(4\text{-carboxy-}2\text{-}[2'\text{-}(4'\text{-carboxypyridyl})]quinoline)_2(NCS)_2]$ has been investigated by Yanagida et al. [13]. They found that the IPCE spectrum extended up to 900 nm. Unfortunately, the maximum IPCE value obtained for this dye is lower (~40%) compared to the N719 (~80%). This is due to the lower LUMO which is 0.24 V below that of N719.

2.3.2. Porphyrin sensitizer

The porphyrin sensitizer also requires a binding group such as carboxylic acid and 8-hydroxylquinoline (HQ) to adsorb efficiently the TiO_2 semiconductor [14]. The linkers containing carboxylic acid or HQ can be located at *β*-positions or *meso*-positions or both (shown in **Figure 5**).

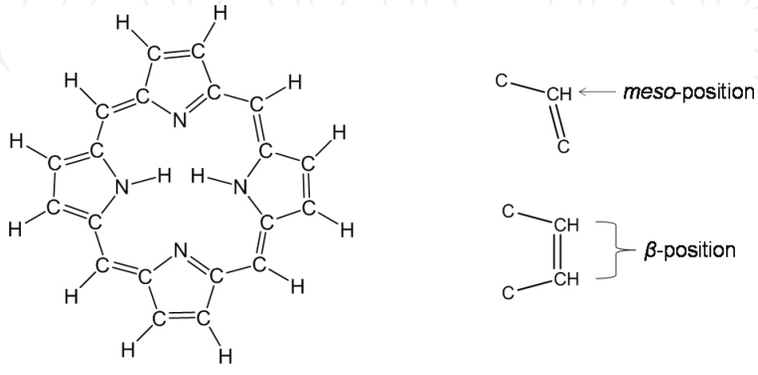

Figure 5. Basic porphyrin structure. The mesoposition is at C—CH═C and β-position is at C—CH═CH—C. The hydrogen at meso- and β-positions will be substituted by functional groups such as diarylamino, fluorene, etc.

Kay and Grätzel were the first to report on DSSC using copper porphyrin [15]. The overall efficiency was 2.6%. The development of porphyrin sensitizers for SSCs gained more attention when Wang et al. [16] reported an efficiency of 5.6% under AM 1.5 illumination using zinc-porphyrin as the sensitizer with the co-adsorbent chenodeoxycholic acid (CDCA). The efficiency was increased to 7.1% reported by the same group for the zinc-porphyrin sensitizer with the aryl group as the electron donor and malonic acid as the acceptor ,which is shown in **Figure 6** [17]. Since then, the research on development of the porphyrin sensitizer increased rapidly. Park et al. [18] have shown that electron injection can be enhanced using two equivalent π-conjugated malonic acid linkers at the β-position. This led to higher J_{sc}.

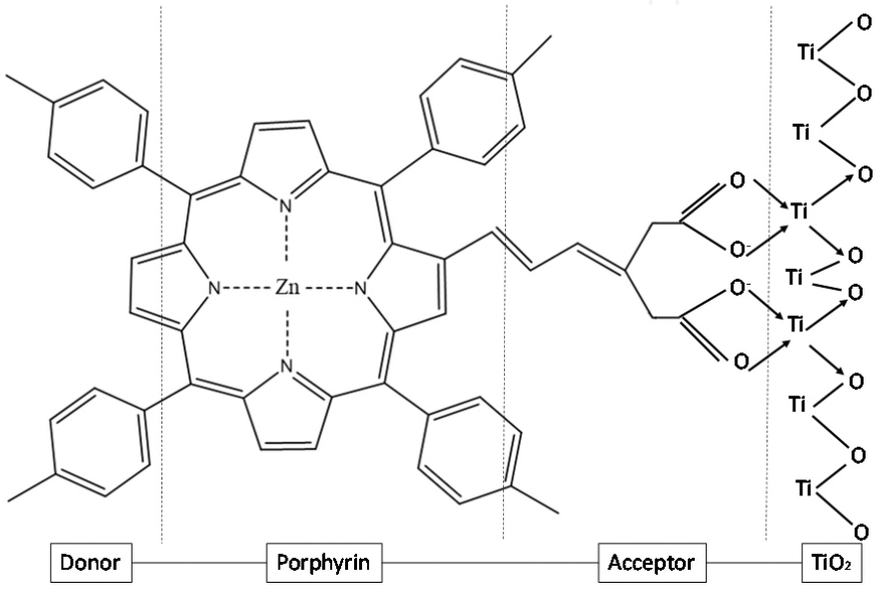

Figure 6. Structure of malonic acid porphyrin substituted at the β-position.

The serious dye aggregation problem for porphyrins on TiO_2 films compared with the ruthenium complexes led to poor DSSC efficiency. The problem was solved by introducing long alkyl chains and 3,5-di-tert-butylphenyl groups to the porphyrin ring at the *meso*-position [19]. By attaching the diarylamino group to the porphyrin ring, the DSSC exhibits an efficiency of 6.0% [20]. The efficiency was further enhanced to 6.8% by attaching two *tert*-butyl groups in the diarylamino group instead of two long alkyl chains (C_6H_{13}) coded as YD2 and co-adsorbed with CDCA. Bessho et al. [21] reported that the efficiency increased up to 11% when a thin reflecting layer of 5 μm thickness was coated on the TiO_2 and sensitized with the YD2 sensitizer.

To further improve the performance of porphyrin based DSSC, light harvesting has to be enhanced which means the HOMO and LUMO energy gap must be decreased. There are two approaches: (1) to fuse or dimerize porphyrins and (2) by coupling a chromophore to the porphyrin ring. Eu et al. [22] have fused two quinoxaline derivatives to the zinc porphyrin to form 5,10,15,20-tetrakis(2,4,6-trimethylphenyl)-6′-carboxyquinoxalino[2, 3-β] porphyrinato-zinc (II) or ZnQMA and 5,10,15, 20-tetrakis(2,4,6-trimethylphenyl)-6′,7′-dicarboxyquinoxali-

no[2, 3-β]porphyrinatozinc (II) or ZnQDA. ZnQMA and ZnQDA based DSSCs exhibit the efficiencies of 5.2% and 4.0% respectively. The IPCE spectrum for both porphyrin sensitizers extended only up to ~700 nm. The fused porphyrin approach has successfully extended the light absorption to wavelengths longer than that in the visible region (~1000 nm) for nickel porphyrins fused with perylene anhydride as reported by Jiao et al. [23]. Unfortunately, the overall efficiency obtained was only 1.36%. The reason for low performance is the dye aggregation that resulted in the LUMO energy to be very close to the TiO_2 CB edge and the short lifespan of the dye excited state.

The introduction of a highly conjugated π-extended chromophore at the *meso*-position can enhance light harvesting of the porphyrin dye. Wu et al. [24] has modified porphyrin by attaching fluorene, acenaphthene and biphenyl to one of the *meso*-positions. A broad IPCE spectrum near 800 nm with stronger response in the 400–500 and 550–750 nm regions were observed for DSSC using these three dyes. They observed that fluorenyl substituents showed the highest efficiency (8.1%). A year before, the same group [25] showed that pyrene-functionalized porphyrin exhibited an efficiency of 10.06% superior to N719 (9.3%). Dye aggregate formation significantly limited the performance of the porphyrin based solar cell. In order to further suppress dye aggregation, a long alkoxy chain zinc porphyrin was employed for protection of the porphyrin core. In 2014, Mathew et al. [26] reported an efficiency as high as 13% for porphyrin-sensitized DSSC. The porphyrin was coded SM315. The mediator used for this DSSC was Co(II/III).

2.3.3. Non-metallic organic dyes

Metal free or non-metallic organic dyes have been studied intensively to replace ruthenium-based sensitizers in DSSC. The metal free organic dyes have a molar extinction coefficient that is usually higher than Ru complexes [27–29]. Metal free dyes have opto-electronic properties that are easily tuned and they are cheaper to produce [30]. The general design principle for dye sensitizer is shown in **Figure 7**.

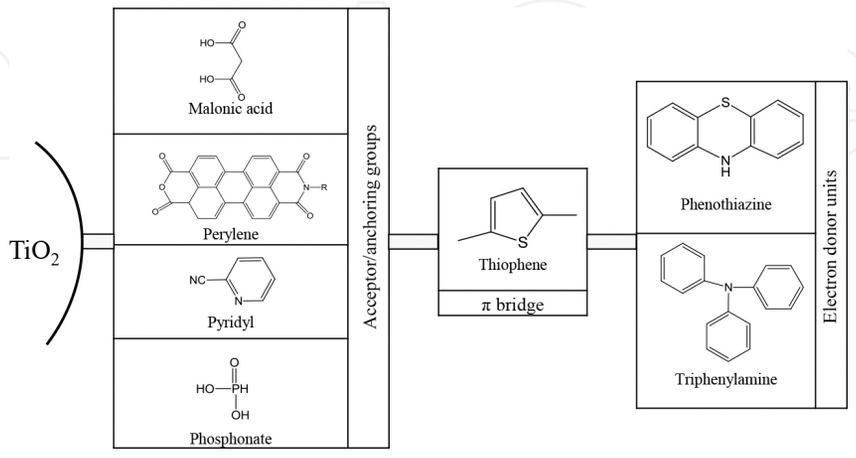

Figure 7. Design structure for non-metallic dye. The electrons from the donor will be transferred to TiO_2 through the π - bridge and the acceptor.

In general, organic dyes can be grouped as neutral and ionic organic dyes. Examples of neutral organic dyes are coumarins, triphenylamine, phenothiazine and indoline. Examples of ionic organic dyes are squarylium, cyanine, hemicyanine and merocyanine.

Tian et al. [31] have synthesized organic dyes with phenothiazine (PTZ) as the electron donor and rhodamine-3-acetic acid or cyanoacrylic acid as the electron acceptor. The DSSC utilizing the dye with cyanoacrylic acid as the anchoring acceptor exhibited 5.5% efficiency. Marszalek et al. [32] reported two novel organic dyes. The dyes comprised of electron donating 10-butyl-(2-methylthio)-10*H*-phenothiazine with and without the vinyl thiophene group (VTP) as the π-bridge. The acceptor used is cyanoacrylic acid. With VTP, the IPCE value observed was up to 80% in the wavelength range between 380 and 750 nm, whereas without VTP, the range was between 380 and 650 nm. This results in higher J_{sc} and efficiency for the DSSC using the VTP attached dye. The photocurrent density enhanced from 11.2 to 15.2 mA/cm^2 and the efficiency reached 7.4%.

Coumarin-based dye is a promising sensitizer for DSSC because it has good photoelectric conversion properties [33]. Wang et al. [33] reported that a DSSC using coumarin dye, 2-cyano-3-(5-{2-[5-(1,1,6,6-tetramethyl-10-oxo-2,3,5,6-tetrahydro-*1H, 4H, 10H*-11-oxa-3a-aza-benzo[*de*] anthracen-9-yl)-thiophen-2-yl]-vinyl}, -thiophen-2-yl)-acrylic acid exhibited an efficiency of 8.2%.

3. Quantum dot-sensitized solar cells (QDSSCs)

As the research on DSSCs progressed, the idea of replacing dyes with QDs emerged. QDs are nano-dimensional structures with a narrow band gap suitable for absorbing light in the visible region. Therefore, when deposited over the mesoporous TiO_2 layer, the excited electrons in the QDs can be transferred to the mesoporous TiO_2. Research on sensitization of a wide band gap semiconductor by using a narrow band gap material such as dye started during the 1960s, but QDs was used for wide band gap semiconductor sensitization for the first time in 1986 by Gerischer et al. [34]. Advancement in research on sensitization led to DSSCs. Based on the highly porous TiO_2 DSSCs introduced by O'Regan and Grätzel [6], QDs were introduced to replace the dye [35–37]. Until now, a lot of research has been geared towards improving QDSSCs performance. The highest efficiency recorded is now around 9% [38, 39].

There are several advantages of inorganic QDs over organic dyes. This is because inorganic QDs are easy to produce and durable [40]. Moreover, the optical band gap of QDs is tuneable [41]. Another special property of QDs is the production of at least two electron-hole pairs per photon with hot electrons. This is due to the impact of ionization in the QD nano-sized semiconducting material [42]. QDs can also reduce dark current and in doing so improve working of the photovoltaic system. This is because the extinction coefficient of QDs is high [43]. The theoretical efficiency for QDSSCs calculated by considering carrier multiplication due to impact of ionization was 44.4% [44].

QDSSCs and DSSCs have a lot of similarities and some differences. The major difference between these two is the sensitizer. QDSSCs utilize nano-sized semiconductor QDs and DSSCs

utilize light absorbing dye. Another difference is material conformity. Some materials that worked effectively in DSSCs are not compatible with QDSSCs and could give a bad impact on the performance of the cells. **Table 1** compares the components for DSSCs and QDSSCs.

Component	QDSSCs	DSSCs
Sensitizer	Sensitizer used is inorganic quantum dots such as CdSe, CdTe, CdS, etc.	Sensitizer include organic dye such as ruthenium based dye, natural dye, etc.
Wide band gap semiconductor	A lot of work on QDSSCs utilized TiO_2 as the one of photoanode components	A lot of work on DSSCs utilized TiO_2 as one of the photoanode components
Electrolyte	Works on QDSSCs, employs the polysulphide redox mediator in the electrolyte due to its stability towards quantum dot	Works on DSSCs employs the iodide based redox mediator in the electrolyte due to its stability towards DSSCs performance
Counter electrode	Metal chalcogenides	Platinum

Table 1. A straightforward comparison between QDSSCs and DSSCs.

3.1. QDSSC structure

Although progress has been made, the efficiency value of QDSSCs has not surpassed that of DSSCs, which is 13% [26]. There is still a lot of improvement to be done in obtaining a better material for QDSSCs. **Figure 8** illustrates schematically the QDSSC device and its components.

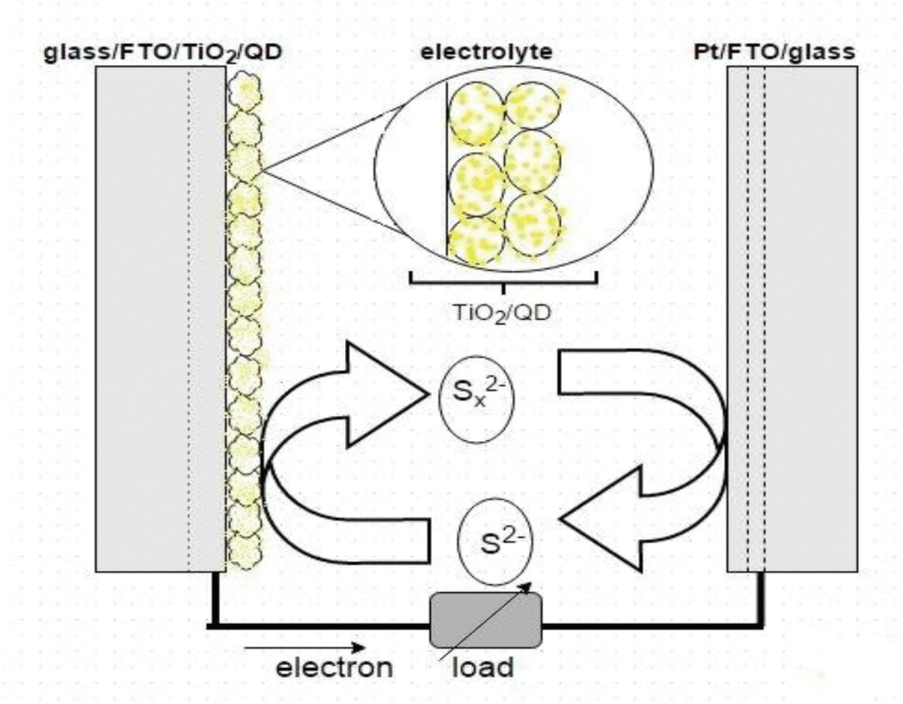

Figure 8. An illustration of QDSSCs with its three main components: photoanode, electrolyte and counter electrode.

3.1.1. Photoanode

In works concerning QDSSCs, very frequently TiO_2 was utilized as the wide band gap semiconductor compared to other oxides. Out of the many QDs chalcogenides, cadmium chalcogenides (CdS, CdSe and CdTe) are most popularly used in QDSSCs [45–47]. Another important component in QDSSC photoanodes is the passivation layer. The passivation layer prevents electron recombination that can improve performance of QDSSCs since the short circuit current density will not be reduced.

Chalcogenides of cadmium can easily be fabricated and have a tuneable band gap that can be achieved by controlling their size [45, 48–50]. CdS, CdSe and CdTe chalcogenide QDs have a band gap 2.3, 1.7 and 1.4 eV, respectively. Hence, incident light in the visible wavelength can be absorbed up to ~540 nm for CdS, ~731 nm for CdSe and ~887 nm for CdTe. **Figure 9** shows the valence band (VB) and conduction bands of cadmium chalcogenide QDs and TiO_2.

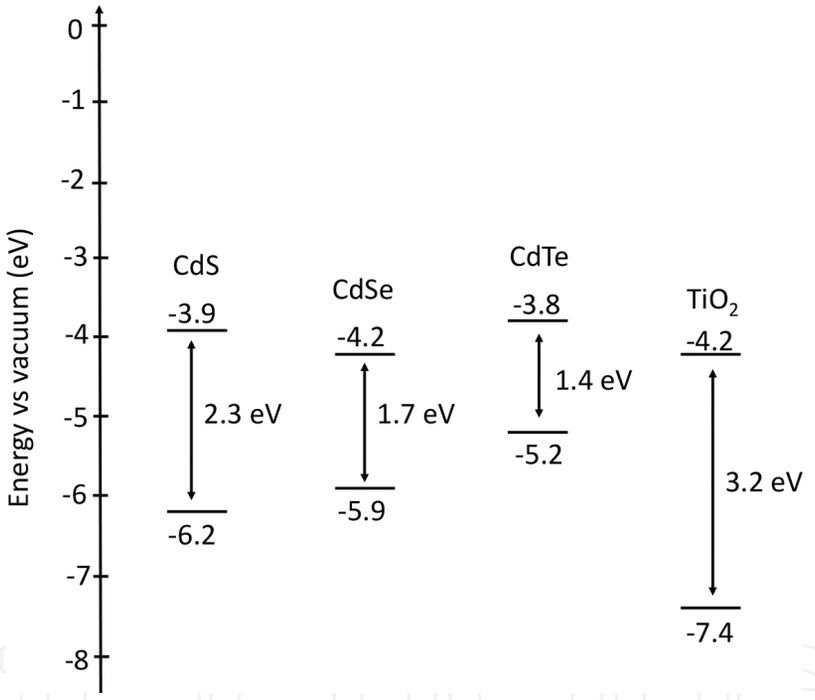

Figure 9. Energy levels of cadmium chalcogenide QDs (CdS, CdSe and CdTe) and TiO_2.

The use of two species of QDs in a single QDSSC has proven to enhance the efficiency, for example, CdS/CdSe, CdTe/CdSe and CdTe/CdS combinations were used as sensitizers [43, 51, 52]. When CdS and CdSe make contact with each other, electron redistribution will occur resulting in the CdS and CdSe band edge to shift to more or less positive potentials, respectively. The shifting of the band edge is referred to Fermi level alignment [43]. This process affects electron injection. The same process also happens in the combinations of CdTe/CdSe and CdTe/CdS. **Figure 10** shows how CdTe/CdSe and CdS/CdSe combinations produce an effective electron injection. Application of co-sensitizing QDs in QDSSCs has shown excellent performance compared to QDSSCs fabricated with a single QD sensitizer [43, 51, 52].

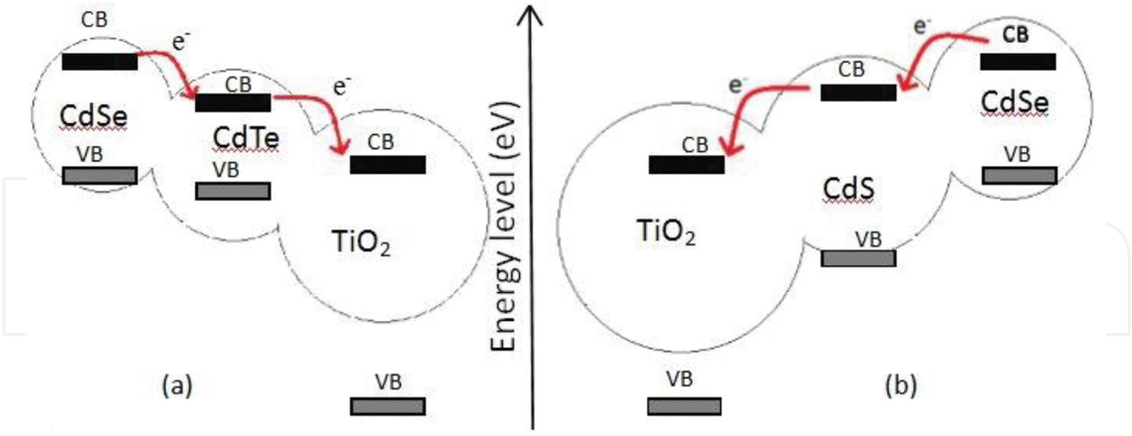

Figure 10. Changing of the band edge level of QDs after electron redistribution of: (a) CdTe/CdSe and (b) CdS/CdSe. This arrangement is necessary for electron injection from CdSe to CB of TiO_2 due to the alignment of the Fermi level.

Although tuning band gap with the size of the QDs is promising in enhancing performance of QDSSCs, this may give rise to stability problem [53]. To avoid this, alloyed cadmium chalcogenide QDs (AB_xC_{1-x}, A = Cd, B and C = S or Se or Te) were used to tailor the band gap of the QDSSCs without having to change the particle size [53, 54]. An example of alloyed cadmium chalcogenide is $CdTe_xS_{1-x}$. The band gap of the $CdTe_xS_{1-x}$ alloyed QD can be adjusted to the range of visible light by changing the tellurium molar ratio and make it exhibit a high potential in photovoltaic application [55]. Another excellent alloyed cadmium chalcogenide used in QDSSCs is $CdSe_xTe_{1-x}$. $CdSe_xTe_{1-x}$has been utilized in QDSSCs by Ren et al. [38] and Yang et al. [39]. Photon-to-electricity efficiency obtained was 9 and 9.4% respectively. Employment of alloyed cadmium chalcogenide in QDSSCs have a very promising future since it will give a better efficiency value and high stability towards performance of QDSSCs.

Even though QDs have many advantages as a sensitizer compared to organic dyes, the efficiency recorded for QDSSCs is still lower compared to DSSCs. Excited electrons in QDs can take one of three possible routes which are: (1) jump into the TiO_2 conduction band which will be beneficial to the performance of the QDSSCs, (2) relax into the valence band by emitting energy and finally (3) combine with redox mediator ions (recombination process) in the electrolyte which are routes detrimental to the QDSSC performance. To overcome recombination, researchers have QDs coated on the surface with ZnS, SiO_2 and amorphous TiO_2 (am-TiO_2) [38, 56, 57]. Ren et al. [38] have introduced a novel strategy to overcome recombination by implementing three passivation layers am-TiO_2/ZnS/SiO_2 resulting in 9% efficiency. Yang et al. [39] utilized the CdS layer as a passivation layer to the CdSeTe QDs and achieved 9.4% efficiency.

3.1.2. Electrolyte

Another important component in QDSSCs is the electrolyte. The electrolyte in QDSSCs functions as a charge carrier transporter between the photoanode and the counter electrode

done via the redox mediators. The redox species in the electrolyte are also responsible for turning the oxidized QD species by donating an electron to the QDs. In QDSSCs, polysulphide electrolytes with S^{2-}/S_x^{2-} are widely utilized by researchers since they can give good performance and stability [58–60]. Performance of QDSSCs can also be improved by utilization of chemical additives in the polysulphide electrolyte. Park et al. [61] reported that by introducing sodium hydroxide (NaOH) into the polysulphide electrolyte of QDSSCs, V_{oc} and *FF* can be increased.

Due to problems that arise from utilization of liquid electrolytes such as leakage and easy vaporization, researchers have begun to use polymer electrolytes. However, the performance of QDSSCs based on the solid polymer electrolyte [62, 63] is low compared to QDSSCs fabricated with liquid electrolytes. This is because solid state electrolytes suffer from low ionic conductivity. Another alternative to the liquid electrolyte is to use gel polymer electrolytes (GPEs). GPE is very competitive since GPE based QDSSC performance is comparable with QDSSCs fabricated with the liquid electrolyte [64–66]. Kim et al. [65] successfully fabricated CdSe/CdS GPE based QDSSCs with 5.45% efficiency, which is comparable with QDSSCs based on the liquid electrolyte. As the GPE based QDSSCs is comparable with QDSSCs fabricated with the liquid electrolyte, utilization of GPE in QDSSCs will be an advantage in terms of providing stability and overcoming problems that arise from liquid electrolytes.

3.1.3. Counter electrode

The counter electrode is another important component in QDSSCs. Electrons from the photoanode are returned to the QD when the electrons react with the redox ions in the electrolyte. In DSSCs, platinum (Pt) is the best material to be used as the CE due to its high stability and high catalytic activity for the triiodide ion to be reduced into the iodide ion. However, Pt CE does not work for QDSSCs. This is because Pt [67]:

1. is not catalytic to the sulphide ion,

2. restrains the charge transfer to polysulphide ions and

3. can react with sulphur.

Hence, researchers look for alternative materials to be used as the CE such as noble metals, carbon based materials and metal chalcogenides [68]. The highest efficiency are presently exhibited by QDSSCs utilizing copper sulphide (Cu_2S) as the CE (η = 9%) [39].

3.2. Working principle of QDSSC

Basically, QDSSCs working mechanism is identical with DSSCs. TiO_2 is used in the photoanode. Upon light incident, the QD sensitizers absorb photons to excite electrons into its CB (photoexcitation). Electrons in the CB of QDs will be injected to the CB of TiO_2 and oxidized QDs will be regenerated by receiving electron from S^{2-} ions in the electrolyte [69]. From CB of TiO_2, electrons will leave the photoanode, enter the external circuit and reach the counter

electrode where they will be received by S_x^{2-} ions in the electrolyte (S_x^{2-} transforms into S^{2-}).

As the above process continues, electrons will keep moving through the cell and current is produced. **Figure 11** shows the working mechanism of QDSSCs where only electron movement is shown. Red arrows in **Figure 11** indicate the electron movement.

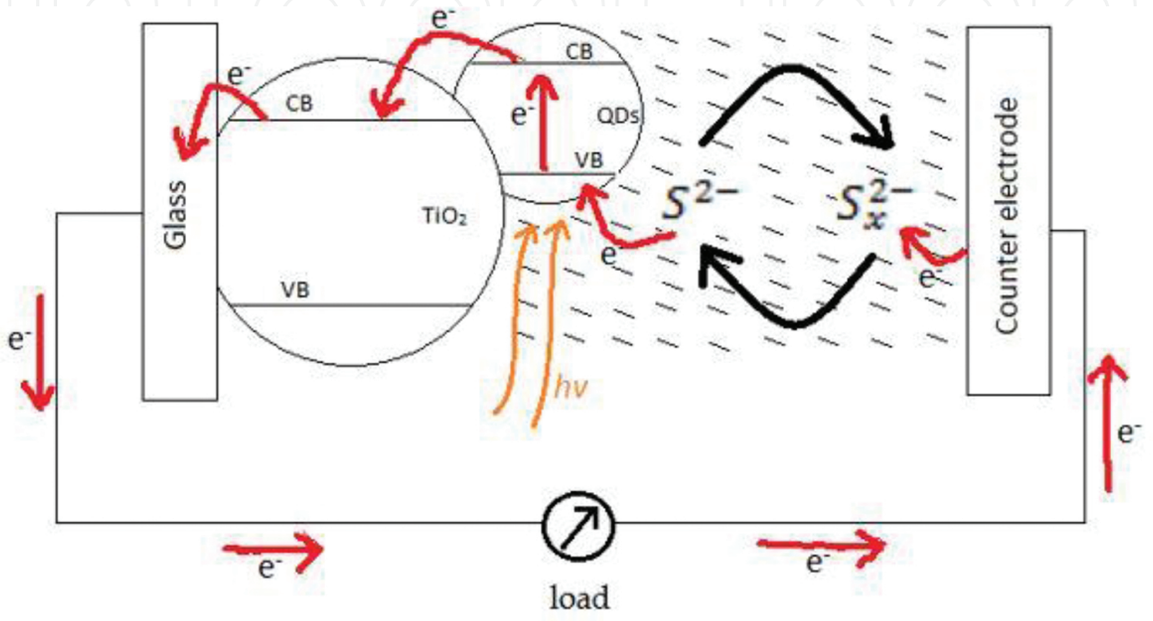

Figure 11. This figure demonstrates the movement of electron starting from QDs excited due to photon absorption.

4. Perovskite-sensitized solar cell

Perovskite is a term for materials that have a similar crystal structure to calcium titanium oxide ($CaTiO_3$), that is, ABX_3 where A and B are cations and X is an anion. A is typically a large cation, such as ethylammonium ($CH_3CH_2NH_3^+$) [70], formamidinium ($NH_2CH{=}NH_2^+$) [71] and methylammonium ($CH_3NH_3^+$) [72]. B is a cation metal of carbon family, such as Ge^{2+}, Sn^{2+} and Pb^{2+} and anion X is a halogen (F, Cl, Br and I).

Perovskite cells are typically fabricated with two structures which are mesoporous and planar structures.

4.1. Mesoporous structure

The mesoporous structure consists of a transparent conducting oxide (TCO) substrate coated with an oxide semiconductor compact layer, mesoporous metal oxide (e.g. TiO_2, Al_2O_3), perovskite sensitizer, hole conductor and gold conductor.

Kojima et al. [73] reported the first perovskite material ($CH_3NH_3PbBr_3$ and $CH_3NH_3PbI_3$) used as a sensitizer in photoelectrochemical cells. The cell consists of mesoporous TiO_2 film having 8–12 μm thickness, iodide/triiodide redox couple liquid electrolyte and platinum counter electrode. The band gap $CH_3NH_3PbBr_3$ is 1.78 eV and that of $CH_3NH_3PbI_3$ is 1.55 eV. They have reported that the solar cells using $CH_3NH_3PbBr_3$ and $CH_3NH_3PbI_3$ sensitizers exhibit the efficiencies of 3.13 and 3.81%, respectively. TiO_2 sensitized with orthorhombic $(CH_3CH_2NH_3)PbI_3$ has been reported by Im et al. [70] to have an optical band gap of 2.2 eV. The cell using the $(CH_3CH_2NH_3)PbI_3$ sensitizer and the electrolyte with the iodide/triiodide redox mediator exhibits an efficiency of 2.4%. Based on the work done by Kojima et al. [73], Im et al. [74] have investigated the effect of TiO_2 film thickness on perovskite photovoltaic performance. The cell with 8.6 μm thick TiO_2 film exhibits an efficiency of 3.37% comparable with that of Kojima et al. [73]. The performance of the cell increases when the TiO_2 film thickness decreases. The cell with 3.6 μm thick TiO_2 film exhibits an efficiency of 6.2%. Unfortunately, the cell exhibited poor stability due to perovskite decomposition and degraded within minutes. In 2012, the stability of $CH_3NH_3PbI_3$-sensitized solar cell over 500 h has been reported by Kim et al. [72]. They have substituted the liquid electrolyte that was previously tried by Kojima et al. [73] with a solid state hole transport layer (*spiro*-MeOTAD). Their results also support the work done by Im et al. [74] where the efficiency of the cell increased with the decrease of TiO_2 thickness and the highest efficiency of 9.7% observed for the cell having TiO_2 thickness of 0.6 μm. Based on the impedance spectroscopy results, they found that the dark current and electron transport resistance increased with the increase in TiO_2 film thickness. Koh et al. [71] have synthesized a novel $(NH_2CH{=}NH_2)PbI_3$ perovskite with an energy band gap of 1.47 eV. Although the band gap of $(NH_2CH{=}NH_2)PbI_3$ is smaller compared to that of $CH_3NH_3PbI_3$, the efficiency of the cell is only 4.3%. The low efficiency is attributed to the energy level mismatch between TiO_2 and the perovskite. The working mechanism of the above perovskite photovoltaics is expected to be similar to DSSC (**Figure 12a**) where the perovskite absorbs light, injects electrons to the CB of TiO_2 and holes to the solid state hole transport material (HTM).

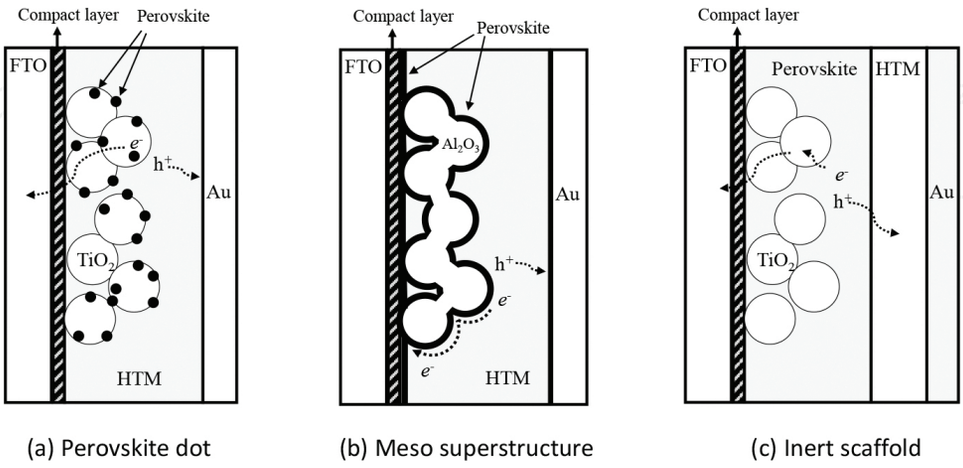

Figure 12. Mesoporous structure of perovskite solar cell. (a) Perovskite dot: the structure is similar to DSSC. (b) Meso superstructure: the CB of the oxide semiconductor used is higher than the perovskite material and its surface is coated completely. (c) Inert scaffold: the perovskite fills the pores and makes a thin layer on the top of TiO_2.

Lee et al. [75] have constructed a meso superstructure (**Figure 12b**) of an organometal halide perovskite solar cell. This structure can be obtained by controlling the perovskite precursor concentration. The cell consists of mesoporous n-type TiO_2, $CH_3NH_3PbI_3Cl$ and p-type *spiro*-OMeTAD hole conductor. The cell exhibited an efficiency of 7.6%. The efficiency was increased up to 10.9% with the substitution of TiO_2 with Al_2O_3. For the TiO_2 based perovskite solar cell, electrons in the $CH_3NH_3PbI_3Cl$ sensitizer is expected to be injected to the CB of TiO_2 and transported to the FTO electrode whereas holes will be transferred to the *spiro*-OMeTAD layer. In the case of Al_2O_3-based perovskite solar cell, electrons will be transferred through the perovskite because Al_2O_3 has a wider band gap (7–9 eV) and the CB of Al_2O_3 is higher than $CH_3NH_3PbI_3Cl$. This shows that the perovskite layer functions as an absorber and n-type component. The authors also reported that the electron diffusion through perovskite is faster than in TiO_2 and thus leads to a higher efficiency. The Mesoporous scaffold structure where the perovskite filled up the pores and formed a dense layer on top of mesoporous TiO_2 (**Figure 12c**) has been reported by Heo et al. [76]. For this structure, they have shown that the $CH_3NH_3PbI_3$ can act both as a light harvester and as a hole conductor which was also previously reported by Etgar et al. [77]. The excitation of $CH_3NH_3PbI_3$ produced excitons, which was then dissociated via electron injection at the $TiO_2/CH_3NH_3PbI_3$ interface. Injected electrons are transported to the FTO electrode through the TiO_2 network and holes are transported through perovskite to HTM and finally arrive at the Au electrode. The highest efficiency reported by Heo et al. [76] was 12% for the cell configuration of FTO/mesoporous TiO_2 layer/$CH_3NH_3PbI_3$/poly-triarylamine/Au. By blending TiO_2 nano-particles with nanorods, the efficiency increased up to 15% [78].

4.2. Planar structure

The planar perovskite solar cell architecture is similar to the mesoporous structure except for the mesoporous metal oxide.

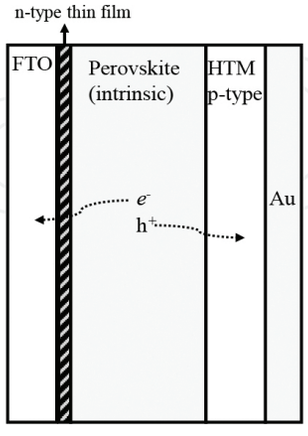

Figure 13. Planar structure of perovskite solar cell. No mesoporous structure involved.

Lee et al. [75] have shown that the perovskite photovoltaic system can still function without the non-blocking TiO_2 layer. Hence, the planar p-i-n and the p-n junction perovskite structures

are possible to construct. **Figure 13** shows an example of the p-i-n junction perovskite solar cell, which consists of an n-type compact metal oxide thin layer, intrinsic perovskite layer and p-type HTM layer. This structure has been demonstrated by Liu et al. [79] using n-type TiO_2 compact layer, perovskite $CH_3NH_3PbI_{3-x}Cl_x$ and p-type *spiro*-MeOTAD. They used vapour deposition technique to deposit the perovskite layer and reported an efficiency of 15%. Murugadoss et al. [80] have reported an efficiency of 8.38% for the $CH_3NH_3PbI_3$ perovskite solar cell using SnO_2 as the compact layer and the CuSCN as hole conductor. The first hole conductor free perovskite solar cell with an efficiency of 5.5% was reported by Etgar et al. [77]. The cell configuration was FTO/compact TiO_2/TiO_2 nanosheet/Perovskite/Au. A year later, the efficiency increased to 8% as reported by the same group after the TiO_2 nanosheet has been replaced with thinner TiO_2 film [81].

4.3. Lead free perovskite solar cell

Perovskite cells have shown a high efficiency of 21%. The perovskite material is very absorptive and moisture sensitive. The main problems are stability and lifetime. Perovskite solar cells are even less stable than organic polymer photovoltaics. Lead is also poisonous and has to be substituted by some other friendlier materials, like Sn. These are among the main challenges faced by researchers. The absorption of tin halide perovskite has been reported up to 1000 nm [82]. By partially substituting lead with tin ($CH_3NH_3Sn_xPb_{1-x}I_3$), the band gap can be reduced by increasing the Sn concentration. Hao et. al [83] has reported an efficiency of 7.37% for $CH_3NH_3Sn_{0.25}Pb_{0.75}I_3$ and 5.44% for $CH_3NH_3SnI_3$ perovskite solar cell. Germanium (Ge^{2+}) perovskites of the form, $CsGeX_3$ (X = Cl^-, Br^-, I^-) with a rhombohedral structure and *R*3*m* symmetry is another candidate for perovskite photovoltaics. However, the maximum efficiency of 3.2% is still far below the performance of $CH_3NH_3PbI_3$ perovskite. Orthorhombic $(C_4H_9NH_3)_2GeI_4$ is another variation of Ge-perovskite. This material shows a photoluminescence signal in the red. Stability is still an issue of concern.

5. Summary

The third-generation-sensitized solar cells have proved that they have the potential to compete with the conventional silicon based photovoltaics. The use of cheap materials with high performance make third-generation-sensitized solar cells a bright candidate as a future photovoltaic technology compared to other third-generation solar cells. The sensitized photovoltaic started with the emergence of DSSC using mesoporous nanocrystalline TiO_2 sensitized with the ruthenium based dye molecule. Since then, the molecular engineering of the dye molecules are extensively studied to improve the DSSC performance. The sensitizer used in the photovoltaic device evolved from organic (dye) to inorganic (quantum dot) and hybrid organic-inorganic (perovskite) sensitizer. The tuneable energy band gap of quantum dots enables them to produce multiple electron-hole pairs per photon. The progress in the performance of perovskite solar cells is very promising. In the beginning, the efficiency of the perovskite solar cell was less than 4%. The efficient reached around 20% within less than 10 years. However, the stability and toxicity issues of lead have to be solved before they can be

commercialized. Tin-based perovskite solar cell is already under investigation to replace the toxic lead.

Acknowledgements

Authors thank University of Malaya, Malaysian Ministry of Higher Education (MOHE) and Malaysian Ministry of Science, Technology and Innovation (MOSTI) for the UMRG grant no. RP003-13AFR, PRGS grant no. PR001-2014A and Science fund project no. 03-01-03-SF0995.

Author details

Muhammad Ammar Mingsukang, Mohd Hamdi Buraidah and Abdul Kariem Arof*

*Address all correspondence to: akarof@um.edu.my

Department of Physics, Faculty of Science, Centre for Ionics University of Malaya, University of Malaya, Kuala Lumpur, Malaysia

References

[1] Tributsch H: Reaction of excited chlorophyl molecules at electrodes and in photosynthesis. *Photochemistry and Photobiology* 1972, 16(4):261–269.

[2] Carlson DE, Wronski CR: Amorphous silicon solar cell. *Applied Physics Letters* 1976, 28(11):671–673.

[3] Fang J, Wu J, Lu X, Shen Y, Lu Z: Sensitization of nanocrystalline TiO_2 electrode with quantum sized CdSe and ZnTCPc molecules. *Chemical Physics Letters* 1997, 270(1–2): 145–151.

[4] Smestad GP, Gratzel M: Demonstrating electron transfer and nanotechnology: A natural dye-sensitized nanocrystalline energy converter. *Journal of Chemical Education* 1998, 75(6):752.

[5] Desilvestro J, Grätzel M, Kavan L, Moser J, Augustynski J: Highly efficient sensitization of titanium dioxide. *Journal of the American Chemical Society* 1985, 107(10):2988–2990.

[6] O'Regan' B, Grätzel M: A low-cost, high-efficiency solar cell based on dye-sensitized colloidal TiO_2 films. *Nature* 1991, 353(6346):737–740.

[7] Nazeeruddin MK, Kay A, Rodicio I, Humphry-Baker R, Mueller E, Liska P, Vlachopoulos N, Graetzel M: Conversion of light to electricity by cis-X2bis(2,2'-bipyridyl-4,4'-dicarboxylate)ruthenium(II) charge-transfer sensitizers (X = Cl^-, Br^-, I^-, CN^-, and SCN^-) on

nanocrystalline titanium dioxide electrodes. *Journal of the American Chemical Society* 1993, 115(14):6382–6390.

[8] Bryant G, Fergusson J, Powell H: Charge-transfer and intraligand electronic spectra of bipyridyl complexes of iron, ruthenium, and osmium. I. Bivalent complexes. *Australian Journal of Chemistry* 1971, 24(2):257–273.

[9] Nazeeruddin MK, Pechy P, Gratzel M: Efficient panchromatic sensitization of nanocrystalline TiO_2 films by a black dye based on a trithiocyanato-ruthenium complex. *Chemical Communications* 1997(18):1705–1706.

[10] Hagfeldt A, Grätzel M: Molecular photovoltaics. *Accounts of Chemical Research* 2000, 33(5):269–277.

[11] Nazeeruddin MK, Zakeeruddin SM, Humphry-Baker R, Jirousek M, Liska P, Vlachopoulos N, Shklover V, Fischer C-H, Grätzel M: Acid–base equilibria of (2,2′-bipyridyl-4,4′-dicarboxylic acid)ruthenium(II) complexes and the effect of protonation on charge-transfer sensitization of nanocrystalline titania. *Inorganic Chemistry* 1999, 38(26): 6298–6305.

[12] Islam A, Sugihara H, Singh LP, Hara K, Katoh R, Nagawa Y, Yanagida M, Takahashi Y, Murata S, Arakawa H: Synthesis and photophysical properties of ruthenium(II) charge transfer sensitizers containing 4,4′-dicarboxy-2,2′-biquinoline and 5,8-dicarboxy-6,7-dihydro-dibenzo[1,10]-phenanthroline. *Inorganica Chimica Acta* 2001, 322(1–2):7–16.

[13] Yanagida M, Yamaguchi T, Kurashige M, Hara K, Katoh R, Sugihara H, Arakawa H: Panchromatic sensitization of nanocrystalline TiO_2 with cis-bis(4-carboxy-2-[2′-(4′-carboxypyridyl)]quinoline)bis(thiocyanato-N)ruthenium(II). *Inorganic Chemistry* 2003, 42(24):7921–7931.

[14] He H, Gurung A, Si L: 8-Hydroxylquinoline as a strong alternative anchoring group for porphyrin-sensitized solar cells. *Chemical Communications* 2012, 48(47):5910–5912.

[15] Kay A, Graetzel M: Artificial photosynthesis. 1. Photosensitization of titania solar cells with chlorophyll derivatives and related natural porphyrins. *The Journal of Physical Chemistry* 1993, 97(23):6272–6277.

[16] Wang Z-S, Sayama K, Sugihara H: Efficient eosin Y dye-sensitized solar cell containing Br-/Br3-electrolyte. *The Journal of Physical Chemistry B* 2005, 109(47):22449–22455.

[17] Campbell WM, Jolley KW, Wagner P, Wagner K, Walsh PJ, Gordon KC, Schmidt-Mende L, Nazeeruddin MK, Wang Q, Grätzel M *et al*: Highly efficient porphyrin sensitizers for dye-sensitized solar cells. *The Journal of Physical Chemistry C* 2007, 111(32):11760–11762.

[18] Park JK, Lee HR, Chen J, Shinokubo H, Osuka A, Kim D: Photoelectrochemical properties of doubly β-functionalized porphyrin sensitizers for dye-sensitized nanocrystalline-TiO_2 solar cells. *The Journal of Physical Chemistry C* 2008, 112(42):16691–16699.

[19] Li L-L, Diau EW-G: Porphyrin-sensitized solar cells. *Chemical Society Reviews* 2013, 42(1): 291–304.

[20] Tan Q, Zhang X, Mao L, Xin G, Zhang S: Novel zinc porphyrin sensitizers for dye-sensitized solar cells: Synthesis and spectral, electrochemical, and photovoltaic properties. *Journal of Molecular Structure* 2013, 1035:400–406.

[21] Bessho T, Zakeeruddin SM, Yeh C-Y, Diau EW-G, Grätzel M: Highly efficient mesoscopic dye-sensitized solar cells based on donor–acceptor-substituted porphyrins. *Angewandte Chemie International Edition* 2010, 49(37):6646–6649.

[22] Eu S, Hayashi S, Umeyama T, Matano Y, Araki Y, Imahori H: Quinoxaline-fused porphyrins for dye-sensitized solar cells. *The Journal of Physical Chemistry C* 2008, 112(11):4396–4405.

[23] Jiao C, Zu N, Huang K-W, Wang P, Wu J: Perylene anhydride fused porphyrins as near-infrared sensitizers for dye-sensitized solar cells. *Organic Letters* 2011, 13(14):3652–3655.

[24] Wu C-H, Pan T-Y, Hong S-H, Wang C-L, Kuo H-H, Chu Y-Y, Diau EW-G, Lin C-Y: A fluorene-modified porphyrin for efficient dye-sensitized solar cells. *Chemical Communications* 2012, 48(36):4329–4331.

[25] Wang C-L, Chang Y-C, Lan C-M, Lo C-F, Wei-Guang Diau E, Lin C-Y: Enhanced light harvesting with [small pi]-conjugated cyclic aromatic hydrocarbons for porphyrin-sensitized solar cells. *Energy & Environmental Science* 2011, 4(5):1788–1795.

[26] Mathew S, Yella A, Gao P, Humphry-Baker R, CurchodBasile FE, Ashari-Astani N, Tavernelli I, Rothlisberger U, Nazeeruddin Md K, Grätzel M: Dye-sensitized solar cells with 13% efficiency achieved through the molecular engineering of porphyrin sensitizers. *Nature Chemistry* 2014, 6(3):242-247.

[27] Wang Z-S, Li F-Y, Huang C-H, Wang L, Wei M, Jin L-P, Li N-Q: Photoelectric conversion properties of nanocrystalline TiO_2 electrodes sensitized with hemicyanine derivatives. *The Journal of Physical Chemistry B* 2000, 104(41):9676–9682.

[28] Wang Z-S, Li F-Y, Huang C-H: Photocurrent enhancement of hemicyanine dyes containing RSO_3-group through treating TiO_2 films with hydrochloric acid. *The Journal of Physical Chemistry B* 2001, 105(38):9210–9217.

[29] Ehret A, Stuhl L, Spitler MT: Spectral sensitization of TiO_2 nanocrystalline electrodes with aggregated cyanine dyes. *The Journal of Physical Chemistry B* 2001, 105(41):9960–9965.

[30] Selopal GS, Wu H-P, Lu J, Chang Y-C, Wang M, Vomiero A, Concina I, Diau EW-G: Metal-free organic dyes for TiO_2 and ZnO dye-sensitized solar cells. *Scientific Reports* 2016, 6:18756.

[31] Tian H, Yang X, Chen R, Pan Y, Li L, Hagfeldt A, Sun L: Phenothiazine derivatives for efficient organic dye-sensitized solar cells. *Chemical Communications* 2007(36):3741–3743.

[32] Marszalek M, Nagane S, Ichake A, Humphry-Baker R, Paul V, Zakeeruddin SM, Gratzel M: Tuning spectral properties of phenothiazine based donor-[small

pi]-acceptor dyes for efficient dye-sensitized solar cells. *Journal of Materials Chemistry* 2012, 22(3):889–894.

[33] Wang ZS, Cui Y, Hara K, Dan-oh Y, Kasada C, Shinpo A: A high-light-harvesting-efficiency coumarin dye for stable dye-sensitized solar cells. *Advanced Materials* 2007, 19(8):1138–1141.

[34] Gerischer H, Lübke M: A particle size effect in the sensitization of TiO_2 electrodes by a CdS deposit. *Journal of Electroanalytical Chemistry and Interfacial Electrochemistry* 1986, 204(1):225–227.

[35] Vogel R, Pohl K, Weller H: Sensitization of highly porous, polycrystalline TiO_2 electrodes by quantum sized CdS. *Chemical Physics Letters* 1990, 174(3):241–246.

[36] Vogel R, Hoyer P, Weller H: Quantum-sized PbS, CdS, Ag_2S, Sb_2S_3, and Bi_2S_3 particles as sensitizers for various nanoporous wide-bandgap semiconductors. *The Journal of Physical Chemistry* 1994, 98(12):3183–3188.

[37] Liu D, Kamat PV: Photoelectrochemical behavior of thin cadmium selenide and coupled titania/cadmium selenide semiconductor films. *The Journal of Physical Chemistry* 1993, 97(41):10769–10773.

[38] Ren Z, Wang J, Pan Z, Zhao K, Zhang H, Li Y, Zhao Y, Mora-Sero I, Bisquert J, Zhong X: Amorphous TiO_2 buffer layer boosts efficiency of quantum dot sensitized solar cells to over 9%. *Chemistry of Materials* 2015, 27(24):8398–8405.

[39] Yang J, Wang J, Zhao K, Izuishi T, Li Y, Shen Q, Zhong X: CdSeTe/CdS type-I core/shell quantum dot sensitized solar cells with efficiency over 9%. *The Journal of Physical Chemistry C* 2015, 119(52):28800-28808.

[40] Lee H, Leventis HC, Moon S-J, Chen P, Ito S, Haque SA, Torres T, Nüesch F, Geiger T, Zakeeruddin SM *et al*: PbS and CdS quantum dot-sensitized solid-state solar cells: "old concepts, new results". *Advanced Functional Materials* 2009, 19(17):2735–2742.

[41] Chang C-H, Lee Y-L: Chemical bath deposition of CdS quantum dots onto mesoscopic TiO_2 films for application in quantum-dot-sensitized solar cells. *Applied Physics Letters* 2007, 91(5):053503.

[42] Nozik AJ: Exciton multiplication and relaxation dynamics in quantum dots: Applications to ultrahigh-efficiency solar photon conversion. *Inorganic Chemistry* 2005, 44(20): 6893–6899.

[43] Lee Y-L, Lo Y-S: Highly efficient quantum-dot-sensitized solar cell based on co-sensitization of CdS/CdSe. *Advanced Functional Materials* 2009, 19(4):604–609.

[44] Hanna MC, Nozik AJ: Solar conversion efficiency of photovoltaic and photoelectrolysis cells with carrier multiplication absorbers. *Journal of Applied Physics* 2006, 100(7):074510.

[45] Jun HK, Careem MA, Arof AK: Quantum dot-sensitized solar cells—perspective and recent developments: A review of Cd chalcogenide quantum dots as sensitizers. *Renewable and Sustainable Energy Reviews* 2013, 22:148–167.

[46] Peter LM: The Grätzel cell: Where next? *The Journal of Physical Chemistry Letters* 2011, 2(15):1861–1867.

[47] Rhee JH, Chung C-C, Diau EW-G: A perspective of mesoscopic solar cells based on metal chalcogenide quantum dots and organometal-halide perovskites. *NPG Asia Mater* 2013, 5:e68.

[48] Yu-Jen S, Yuh-Lang L: Assembly of CdS quantum dots onto mesoscopic TiO_2 films for quantum dot-sensitized solar cell applications. *Nanotechnology* 2008, 19(4):045602.

[49] Barcelo I, Campina JM, Lana-Villarreal T, Gomez R: A solid-state CdSe quantum dot sensitized solar cell based on a quaterthiophene as a hole transporting material. *Physical Chemistry Chemical Physics* 2012, 14(16):5801–5807.

[50] Shen X, Jia J, Lin Y, Zhou X: Enhanced performance of CdTe quantum dot sensitized solar cell via anion exchanges. *Journal of Power Sources* 2015, 277:215–221.

[51] McElroy N, Page RC, Espinbarro-Valazquez D, Lewis E, Haigh S, O'Brien P, Binks DJ: Comparison of solar cells sensitised by CdTe/CdSe and CdSe/CdTe core/shell colloidal quantum dots with and without a CdS outer layer. *Thin Solid Films* 2014, 560:65–70.

[52] Yu X-Y, Lei B-X, Kuang D-B, Su C-Y: Highly efficient CdTe/CdS quantum dot sensitized solar cells fabricated by a one-step linker assisted chemical bath deposition. *Chemical Science* 2011, 2(7):1396–1400.

[53] Wang Y, Hou Y, Tang A, Feng B, Li Y, Liu J, Teng F: Synthesis and optical properties of composition-tunable and water-soluble $Zn_xCd_{1-x}Te$ alloyed nanocrystals. *Journal of Crystal Growth* 2007, 308(1):19–25.

[54] Bailey RE, Nie S: Alloyed semiconductor quantum dots: Tuning the optical properties without changing the particle size. *Journal of the American Chemical Society* 2003, 125(23): 7100–7106.

[55] Badawi A, Easawi K, Al-Hosiny N, Abdallah S: Alloyed $CdTe_{0.6}S_{0.4}$ quantum dots sensitized TiO_2 electrodes for photovoltaic applications. *Materials Sciences and Applications* 2014, 5(1):6.

[56] Yang S-m, Huang C-h, Zhai J, Wang Z-s, Jiang L: High photostability and quantum yield of nanoporous TiO_2 thin film electrodes co-sensitized with capped sulfides. *Journal of Materials Chemistry* 2002, 12(5):1459–1464.

[57] Liu Z, Miyauchi M, Uemura Y, Cui Y, Hara K, Zhao Z, Sunahara K, Furube A: Enhancing the performance of quantum dots sensitized solar cell by SiO_2 surface coating. *Applied Physics Letters* 2010, 96(23):233107.

[58] Jun HK, Careem MA, Arof AK: A suitable polysulfide electrolyte for CdSe quantum dot-sensitized solar cells. *International Journal of Photoenergy* 2013, 2013:10.

[59] Shalom M, Dor S, Rühle S, Grinis L, Zaban A: Core/CdS quantum dot/shell mesoporous solar cells with improved stability and efficiency using an amorphous TiO_2 coating. *The Journal of Physical Chemistry C* 2009, 113(9):3895–3898.

[60] Lee Y-L, Chang C-H: Efficient polysulfide electrolyte for CdS quantum dot-sensitized solar cells. *Journal of Power Sources* 2008, 185(1):584–588.

[61] Park S, Son M-K, Kim S-K, Jeong M-S, Prabakar K, Kim H-J: The effects of electrolyte additives on the cell performances of CdS/CdSe quantum dot sensitized solar cells. *Korean Journal of Chemical Engineering* 2013, 30(11):2088–2092.

[62] Duan J, Tang Q, Sun Y, He B, Chen H: Solid-state electrolytes from polysulfide integrated polyvinylpyrrolidone for quantum dot-sensitized solar cells. *RSC Advances* 2014, 4(105):60478–60483.

[63] Duan J, Tang Q, He B, Chen H: All-solid-state quantum dot-sensitized solar cell from plastic crystal electrolyte. *RSC Advances* 2015, 5(42):33463–33467.

[64] Chen H-Y, Lin L, Yu X-Y, Qiu K-Q, Lü X-Y, Kuang D-B, Su C-Y: Dextran based highly conductive hydrogel polysulfide electrolyte for efficient quasi-solid-state quantum dot-sensitized solar cells. *Electrochimica Acta* 2013, 92:117–123.

[65] Kim H, Hwang I, Yong K: Highly durable and efficient quantum dot-sensitized solar cells based on oligomer gel electrolytes. *ACS Applied Materials & Interfaces* 2014, 6(14): 11245–11253.

[66] Yu Z, Zhang Q, Qin D, Luo Y, Li D, Shen Q, Toyoda T, Meng Q: Highly efficient quasi-solid-state quantum-dot-sensitized solar cell based on hydrogel electrolytes. *Electrochemistry Communications* 2010, 12(12):1776–1779.

[67] Radich JG, Dwyer R, Kamat PV: Cu_2S reduced graphene oxide composite for high-efficiency quantum dot solar cells. Overcoming the redox limitations of S2–/Sn2– at the counter electrode. *The Journal of Physical Chemistry Letters* 2011, 2(19):2453–2460.

[68] Meng K, Chen G, Thampi KR: Metal chalcogenides as counter electrode materials in quantum dot sensitized solar cells: A perspective. *Journal of Materials Chemistry A* 2015, 3(46):23074–23089.

[69] Yin X, Que W, Fei D, Xie H, He Z: Effect of TiO_2 shell layer prepared by wet-chemical method on the photovoltaic performance of ZnO nanowires arrays-based quantum dot sensitized solar cells. *Electrochimica Acta* 2013, 99:204–210.

[70] Im J-H, Chung J, Kim S-J, Park N-G: Synthesis, structure, and photovoltaic property of a nanocrystalline 2H perovskite-type novel sensitizer $(CH_3CH_2NH_3)PbI_3$. *Nanoscale Research Letters* 2012, 7(1):1–7.

[71] Koh TM, Fu K, Fang Y, Chen S, Sum TC, Mathews N, Mhaisalkar SG, Boix PP, Baikie T: Formamidinium-containing metal-halide: An alternative material for near-IR absorption perovskite solar cells. *The Journal of Physical Chemistry C* 2014, 118(30):16458–16462.

[72] Kim H-S, Lee C-R, Im J-H, Lee K-B, Moehl T, Marchioro A, Moon S-J, Humphry-Baker R, Yum J-H, Moser JE *et al*: Lead iodide perovskite sensitized all-solid-state submicron

thin film mesoscopic solar cell with efficiency exceeding 9%. *Scientific Reports*. 2012; 2: 591.

[73] Kojima A, Teshima K, Shirai Y, Miyasaka T: Organometal halide perovskites as visible-light sensitizers for photovoltaic cells. *Journal of the American Chemical Society* 2009, 131(17):6050–6051.

[74] Im JH, Lee CR, Lee JW, Park SW, Park NG: 6.5% efficient perovskite quantum-dot-sensitized solar cell. *Nanoscale* 2011, 3: 4088–4093

[75] Lee MM, Teuscher J, Miyasaka T, Murakami TN, Snaith HJ: Efficient hybrid solar cells based on meso-superstructured organometal halide perovskites. *Science* 2012, 338(6107):643–647.

[76] Heo JH, Im SH, Noh JH, Mandal TN, Lim C-S, Chang JA, Lee YH, Kim H-j, Sarkar A, Nazeeruddin MK *et al*: Efficient inorganic-organic hybrid heterojunction solar cells containing perovskite compound and polymeric hole conductors. *Nat Photon* 2013, 7(6): 486–491.

[77] Etgar L, Gao P, Xue Z, Peng Q, Chandiran AK, Liu B, Nazeeruddin MK, Grätzel M: Mesoscopic $CH_3NH_3PbI_3/TiO_2$ heterojunction solar cells. *Journal of the American Chemical Society* 2012, 134(42):17396–17399.

[78] Islam N, Yang M, Zhu K, Fan Z: Mesoporous scaffolds based on TiO_2 nanorods and nanoparticles for efficient hybrid perovskite solar cells. *Journal of Materials Chemistry A* 2015, 3(48):24315–24321.

[79] Liu M, Johnston MB, Snaith HJ: Efficient planar heterojunction perovskite solar cells by vapour deposition. *Nature* 2013, 501(7467):395–398.

[80] Murugadoss G, Kanda H, Tanaka S, Nishino H, Ito S, Imahori H, Umeyama T: An efficient electron transport material of tin oxide for planar structure perovskite solar cells. *Journal of Power Sources* 2016, 307:891–897.

[81] Laban WA, Etgar L: Depleted hole conductor-free lead halide iodide heterojunction solar cells. *Energy & Environmental Science* 2013, 6(11):3249–3253.

[82] Mitzi DB, Feild CA, Harrison WTA, Guloy AM: Conducting tin halides with a layered organic-based perovskite structure. *Nature* 1994, 369(6480):467–469.

[83] Hao F, Stoumpos CC, Chang RPH, Kanatzidis MG: Anomalous band gap behavior in mixed Sn and Pb perovskites enables broadening of absorption spectrum in solar cells. *Journal of the American Chemical Society* 2014, 136(22):8094–8099.

IntechOpen